Binding Affinities for Models of Biologically Available Potential Cu(II) Ligands Relevant to Alzheimer's Disease: An ab Initio Study

Gail A. Rickard, Rodolfo Gomez-Balderas, Patrick Brunelle, Duilio F. Raffa, and Arvi Rauk*

Department of Chemistry, University of Calgary, 2500 University Drive NW, Calgary, Alberta, Canada T2N 1N4

Received: May 3, 2005; In Final Form: July 21, 2005

A systematic study of the binding affinities of the model biological ligands X**:** = $(CH_3)_2S$, CH_3S^-, CH_3NH_2, 4-CH_3-imidazole (MeImid), $C_6H_5O^-$, and $CH_3CO_2^-$ to $(NH_3)_i(H_2O)_{3-i}Cu(II)-H_2O$ (i = 3, 2, 1, 0) complexes has been carried out using quantum chemical calculations. Geometries have been obtained at the B3LYP/6-31G(d) level of theory, and binding energies, $\Delta H^\circ_{(g)}$, relative to H_2O as a ligand, have been calculated at the B3LYP/6-311+G(2df,2p)//B3LYP/6-31G(d) level. Solvation effects have been included using the COSMO model, and the relative binding free energies in aqueous solution ($\Delta G^{\circ\prime}_{(aq)}$) have been determined at pH 7 for processes that are pH dependent. CH_3S^- ($\Delta G^{\circ\prime}_{(aq)} = -16.0$ to -53.5 kJ mol^{-1}) and MeImid ($\Delta G^{\circ\prime}_{(aq)} = -18.5$ to -35.2 kJ mol^{-1}) give the largest binding affinities for Cu(II). PhO^- and $(CH_3)_2S$ are poor ligands for Cu(II), $\Delta G^{\circ\prime}_{(aq)} = 20.6$ to -9.7 and 19.8 to -3.7 kJ mol^{-1}, respectively. The binding affinities for CH_3NH_2 range from -0.8 to -15.0 kJ mol^{-1}. $CH_3CO_2^-$ has Cu(II) binding affinities in the ranges $\Delta G^{\circ\prime}_{(aq)} = -13.5$ to -32.4 kJ mol^{-1} if an adjacent OH bond is available for hydrogen bonding and $\Delta G^{\circ\prime}_{(aq)} = 10.1$ to -4.6 kJ mol^{-1} if this interaction is not present. In the context of copper coordination by the Aβ peptide of Alzheimer's disease, the binding affinities suggest preferential binding of Cu(II) to the three histidine residues plus a lysine or the N-terminus. For a 3N1O Cu(II) ligand arrangement, it is more probable that the oxygen ligand comes from an aspartate/glutamate residue side chain than from the tyrosine at position 10. Methionine appears unlikely to be a Cu(II) ligand in Aβ.

Introduction

Alzheimer's disease (AD) is characterized by the deposition of brain plaques whose main constituents are aggregates of the amyloid-beta peptide (Aβ).[1] Aβ is a 40−42 residue peptide that is thought to induce oxidative stress in the AD brain that leads to peptide oxidation and lipid peroxidation and results in neuronal death.[2] There is significant evidence that transition metals play an important role in the neurotoxicity of Aβ. Elevated levels of copper, zinc, and iron have been found in amyloid plaque deposits in AD brains.[3] Complexation of Cu^{2+} and Zn^{2+} with Aβ induces aggregation of the peptide,[4−6] while the potential redox activity of the Cu(II)/Aβ complex has been implicated in the production of reactive oxygen species (ROS) and subsequent neurotoxicity.[7−9]

Many determinations of the binding affinity of Cu^{2+} for portions of the Aβ peptide of varying lengths have been performed. Early studies on Aβ1−40 and Aβ1−42 produced Cu^{2+} binding affinities on the order of log $K \approx 6$.[6,10] A more recent investigation[11] found both high- and low-affinity sites for Aβ1−40 and Aβ1−42 with Cu^{2+}. At pH 7.4 in vitro, the low-affinity sites for Aβ1−40 and Aβ1−42 exhibit similar binding affinities for Cu^{2+}, log $K = 7.9$ and 8.3, respectively. However, Aβ1−42 has been reported to have a much greater affinity for Cu^{2+} in the high-affinity site than Aβ1−40, log $K = 17.2$ (Aβ1−42) versus 10.3 (Aβ1−40). The Cu^{2+} binding affinity therefore appears to be sensitive to the peptide environment, as is further evidenced by the $6.3 < \log K < 8.8$ value obtained for Aβ1−28.[12]

The nature of the Cu^{2+} binding site in Aβ is still the subject of debate in the literature. It is generally agreed that Aβ forms a square planar coordination geometry with Cu^{2+},[13] with the histidines at positions 13, 14, and possibly 6, filling the majority of the coordination sites on the copper.[12] Evidence is mounting that the N-terminus is also important for copper binding to Aβ.[12,14,15] Agreement therefore exists that three of the four Cu^{2+} ligands in Aβ are nitrogen-based. Controversy essentially arises over whether the ligand in the fourth coordination site is nitrogen- or oxygen-based. Electron paramagnetic resonanace (EPR) parameters indicate a 3N1O ligand arrangement of the copper at physiological pH.[5,8,12−14] Although the oxygen ligand has not been definitively identified, it has been postulated that it is the side chain of the tyrosine at position 10 in Aβ.[16,17] However, mutation of Tyr10 to Phe does not change the EPR spectrum of Cu(II)/Aβ, indicating that tyrosine is not bound to copper in the native Cu(II)/Aβ complex.[14] The lack of Tyr10 binding to copper has also been shown via ^{1}H NMR, Raman spectra, and oxidation experiments.[12,15,18,19] The oxygen ligand may therefore come from another source, such as a water molecule, a backbone carbonyl, or from a glutamate or aspartate residue side chain. EPR studies on Cu(II)/Aβ complexes with isotopically labeled water indicate that a hydration water molecule does not fill the fourth Cu^{2+} coordination site.[14] The likelihood of a carbonyl or carboxylate oxygen being the fourth copper ligand in Aβ has not been thoroughly investigated experimentally. However, ^{1}H NMR of Cu(II)/Aβ in a membrane-mimetic environment did show broadening of the peaks associated with the Asp7, Tyr10, and Gln11, as well as for the His residue side chains compared to the copper-free peptide.[5] In addition, oxidation products of Cu(II)/Aβ(1−16) indicated that

* E-mail: rauk@ucalgary.ca. Phone: 1-403-220-6247. Fax: 1-403-289-9488.

10.1021/jp052303r CCC: $30.25
Published on Web 08/26/2005

the oxygen ligand may come from the carboxylate group of the Asp1 residue.[15] The participation of a carbonyl oxygen has also been mentioned in connection with Cu^{2+} binding to Aβ in senile plaque cores from Raman spectra.[19]

An alternative, 4N, ligand arrangement in the Cu(II)/Aβ complex has been proposed. Raman spectra of soluble Aβ(1−40) indicate binding to copper through histidine residues and to one or more deprotonated amide nitrogens of the peptide main chain.[16] However, a more recent study using circular dichroism (CD) spectra of analogues of Aβ(1−28) implicated all three histidine residues and the N-terminal amino group in the coordination of Cu^{2+}.[12]

The neurotoxicity of Aβ has been linked to oxidative stress induced by the peptide, via pathways that involve the reduction of Cu(II) and the production of ROS such as H_2O_2. The mechanisms of Cu(II) reduction in Aβ are still uncertain, but experimental data indicate that the methionine (Met35) in Aβ is oxidized during the process.[20−22] At present, there are no reports of the methionine as a ligand of the Cu^{2+} in the Cu(II)/Aβ complex, leaving the mechanism of the electron transfer from sulfur to copper unclear. As well as nitrogen and oxygen ligands bound to copper in proteins, sulfur ligands are also commonly found in the copper coordination sphere in biological systems. In many cases, the sulfur is part of a cysteine, but the sulfur from a methionine residue is also often ligated to copper. However, it should be noted that for methionine ligation the proteins involved are mainly blue copper proteins that have type-1 copper centers, with the methionine in an axial position and a Cu−S distance of ∼3 Å.[23,24] An alternative arrangement is seen for peptidylglycine α-hydroxylating monooxygenase, which has a tetracoordinate Cu(II) center with a ligated methionine in a tetrahedral copper arrangement.[25,26] Thus, methionine ligation in copper proteins seems to occur when the copper binding environment has a Cu(I) type geometry. This is not the case in Aβ, so methionine ligation in the Cu(II)/Aβ complex is unlikely, but it may be that methionine coordinates transiently to Cu(II) in order for electron transfer to occur. Homocysteine has also been implicated in AD[27−29] and has been shown to potentiate copper and Aβ mediated toxicity in neuronal cultures through oxidative damage.[30]

The lack of a definitive description of the specific nature and arrangement of the ligands in the Cu(II)/Aβ complex from experimental data has prompted the current study. The aim of the investigation has been to compute the binding affinities of potential Cu(II) ligands present in Aβ using quantum chemical calculations. The data obtained have been used to gain insight into the relative binding affinities of the various ligands in biological copper−protein systems and, in particular, in the Aβ peptide. Model Aβ ligands, plus methyl thiolate to represent cysteine or homocysteine, and small copper complexes have been used.

Theoretical Methods

Ab initio calculations were performed with the *Gaussian 03* suite of programs.[31] MOLDEN 4.0[32] and MOLEKEL 4.0[33] visualization programs were extensively employed. Geometry optimization and harmonic frequency analysis were carried out at the B3LYP/6-31G(d) level of theory. Zero-point energies were scaled by a factor of 0.9806.[34] Single-point energy calculations were performed on the optimized geometries at the B3LYP/6-311+G(2df,2p) level to obtain more accurate enthalpy changes for the reactions under investigation. Since we were examining reactions occurring in aqueous solution, the entropies taken from the *Gaussian 03* output were converted from 1 atm to 1 M by subtracting R ln(24.46) J K^{-1} mol^{-1} to account for the volume change between the two states at 298 K.

Solvation effects were modeled using single-point energy calculations at the B3LYP/6-31G(d) level, with water as the solvent, and the self-consistent reaction field polarizable continuum model, COSMO,[35,36] as implemented in *Gaussian 03* (SCRF-CPCM).[37,38] To define the solvent cavity, the atomic radii were adjusted to fit the gaseous-phase molecular 0.001 electrons $bohr^{-3}$ isodensity surface of the solute.[39,40] Experimental free energies of solvation have been used for H_2O (ΔG_{solv} = −26.4 kJ mol^{-1})[41] and H^+ (ΔG_{solv} = −1107 kJ mol^{-1}).[42] An addition of RT ln(55.6) kJ mol^{-1} was made to the free energy of solvation of water, since liquid water is 55.6 M.

Empirical corrections have been made to the calculated free energies of solvation, ΔG_{solv}, for the ligand molecules X**:** and XH where they are charged. The solvation procedure described above has a tendency to overestimate ΔG_{solv} for positively charged species and underestimate ΔG_{solv} for negatively charged species where specific hydrogen bonding is an essential part of the free energy of solvation.[43] The empirical corrections were determined using the procedure outlined in ref 43. This utilizes experimental pK_a's, as they provide a sensitive measure of relative free energies in aqueous solution that can be compared with calculated values.

The primary thermodynamic data for all species considered are reported in Table S1 (Supporting Information). Numerical data for all processes described below can be found in Tables S3−S5 in the Supporting Information. The free energies of reaction in aqueous solution calculated at pH 7 are shown graphically in the paper.

Results and Discussion

The Cu(II) complexes investigated here are four-coordinate species with one coordination site filled by a model ligand X**:** where X**:** = $(CH_3)_2S$, CH_3S^-, NH_3, CH_3NH_2, 4-CH_3-imidazole (MeImid), $C_6H_5O^-$ (PhO^-), and $CH_3CO_2^-$. The remaining three coordination sites are taken by water or ammonia molecules in all possible combinations from Cu(II)$(NH_3)_3$X to Cu(II)$(H_2O)_3$X. Additionally, the Cu(II)$(H_2O)_4$ species has been used to represent a hydrated Cu^{2+} ion.

The ligands X**:** have been chosen as models for various amino acid residue side chains that are potential copper ligands in peptides and more specifically are present in Aβ. $(CH_3)_2S$ is a model for a methionine side chain, CH_3NH_2 for either a lysine or the N-terminus of a peptide, MeImid is a model for histidine, and PhO^- for tyrosine. Acetate, $CH_3CO_2^-$, models the side chains of glutamic or aspartic acid. CH_3S^- is a model for cysteine and homocysteine. While neither cysteine nor homocysteine is present in Aβ, the latter has been implicated in Alzheimer's disease.[27−29] Cysteine is commonly found as part of the Cu(II) coordination sphere in blue copper proteins where the copper is in a Cu(I)-like geometry.[23,24] Cu/Zn superoxide dismutase with H46C and H120C mutations produced type-2 tetragonal copper centers with cysteine ligated to Cu(II).[44,45] The H117G mutation of the blue copper protein azurin also yields a type-2 Cu−cysteinate complex.[45,46] It should be noted that experimentally it is very difficult to form stable small Cu(II)−cysteine/thiol complexes because of autocatalytic oxidation of the S^- and reduction of the Cu(II) to Cu(I).[47,48] In a recent kinetic study of the mechanism of the copper-catalyzed autoxidation of mercaptosuccinic acid, Stochel and van Eldik[49] did attribute transiently observed species to Cu(II)-S^- thiolate complexes. The current theoretical investigation of the thiolate, CH_3S^-, as a ligand for a type-2 copper center has been included because of the possible link stated above between homocysteine and Alzheimer's disease. Ammonia has been included as the

TABLE 1: Energy Changes (kJ mol^{-1}): Cu(II)$(H_2O)_x \rightarrow$ Cu(II)$(H_2O)_{x-1}$ + H_2O (reaction 1)[a]

reaction	ΔH (0 K)$_{(g)}$[b]	$\Delta H°$ (298 K)$_{(g)}$[b]	$T\Delta S$	$\Delta G_{(g)}$	$\Delta\Delta G_{solv}$	$\Delta G°_{(aq)}$[c]
$Cu(II)(H_2O)_6 \rightarrow Cu(II)(H_2O)_5 + H_2O$	77.9	80.4	33.0	47.4	−59.5	−12.1
$Cu(II)(H_2O)_5 \rightarrow Cu(II)(H_2O)_4 + H_2O$	98.0	100.5	30.6	69.9	−83.9	−14.0
$Cu(II)(H_2O)_4 \rightarrow Cu(II)(H_2O)_3 + H_2O$	168.0	170.8	33.3	137.5	−98.1	39.4

[a] The standard state for all entropies and gas-phase free energies is 1 M at 298 K. [b] Enthalpies derived from the B3LYP/6-311+G(2df,2p)//B3LYP/6-31G(d) energies. [c] All species are 1 M except H_2O = 55.6 M.

model for a generic nitrogen ligand that may coordinate to copper.

The Cu(II) model ligand complexes have been treated as tetracoordinated species, since the available experimental data for the Cu(II)/Aβ complex suggests that the Cu(II) center is four-coordinate and distorted square planar,[13] although as stated above, the exact nature of the four ligands is still the subject of some controversy in the literature.

The hydrated Cu^{2+} ion is also treated as a tetracoordinated species. Previous theoretical studies on water clusters have shown that the tetracoordinated Cu(II)$(H_2O)_4$ complex most adequately describes the aqueous Cu^{2+} ion,[50,51] rather than the six-coordinate species generally accepted experimentally.[52−54] A more recent combined neutron diffraction and ab initio dynamics study concluded that the five-coordinate species was the most stable.[55] In the current study, we have determined the most stable aqueous Cu^{2+} species using the free energies in aqueous solution for reaction 1, reported in Table 1

$$Cu(II)(H_2O)_x \rightarrow Cu(II)(H_2O)_{x-1} + H_2O \qquad (1)$$

where x = 4, 5, 6. In the gas phase, the hexacoordinated Cu^{2+} ion is the most stable, as evidenced by the positive enthalpy changes shown in Table 1 for losing a water molecule from the Cu(II) coordination sphere. However, the $\Delta\Delta G_{solv}$ for the processes are all negative and for Cu(II)$(H_2O)_6$ and Cu(II)$(H_2O)_5$ are large enough that losing a water molecule from these species becomes exergonic in the aqueous phase. The Cu(II)$(H_2O)_4$ complex is thus the most stable, since adding or removing a water molecule to/from the Cu(II) coordination sphere is an endergonic process in aqueous solution. It therefore appears that the current method provides a better description of the Cu^{2+} aqueous ion as a tetracoordinate, distorted square planar species rather than as a five- or six-coordinate complex with explicit water molecules present in the axial coordination sites. There is a further interesting property of an aqueous Cu^{2+} ion that must be considered, namely that the pK_a for water bound to Cu^{2+} is ~7[56] and may therefore be present as a hydroxide ligand rather than water in biological conditions. However, the loss of a proton was not observed in ab initio dynamics calculations,[50,55] and so for the current study, it has been assumed that water ligands bound to Cu^{2+} are present in their neutral form.

Cu(II) Complexes. The Cu(II) complexes are labeled as number−letter combinations (e.g., **4b**). The number is assigned according to the particular ligand (X**:**) bound to Cu(II) in the order $(CH_3)_2S$ (**1**), CH_3S^- (**2**), NH_3 (**3**), CH_3NH_2 (**4**), MeImid (**5**), PhO^- (**6**), and $CH_3CO_2^-$ (**7**). The letter (**a**−**h**) following the number relates to a specific arrangement of the $i$$NH_3$ and $(3 - i)H_2O$ (i = 3, 2, 1, 0) ligands filling the remaining coordination sites of the Cu(II) (Scheme 1): **a** $(NH_3)_3$, **b** $(NH_3)_2(H_2O)$ (trans), **c** $(NH_3)_2(H_2O)$ (cis1), **d** $(NH_3)_2(H_2O)$ (cis2), **e** $(NH_3)(H_2O)_2$ (trans), **f** $(NH_3)(H_2O)_2$ (cis1), **g** $(NH_3)(H_2O)_2$ (cis2), and **h** $(H_2O)_3$. Thus, **4b**, for example, relates to a methylamine, $2NH_3$, $1H_2O$ complex with the water trans to the ligand CH_3NH_2. For X**:** = $(CH_3)_2S$, PhO^-, or $CH_3CO_2^-$, further differentiation has been made between the cis conformers depending on the orientation of X**:** relative to a NH_3 or H_2O molecule (see Scheme 1). When discussing trends in the binding affinities for a set of Cu(II) complexes that have a particular ligand X**:**, the complexes will be referred to simply by the ligand number, e.g., **1** will represent any complex of $(CH_3)_2S$, **1a**−**1h**.

SCHEME 1: Letter Labeling System for the $(NH_3)_i(H_2O)_{3-i}$Cu(II)−X Complexes

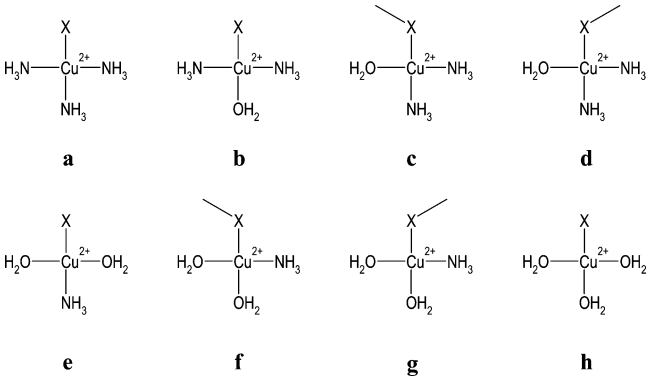

Significant structural parameters and Mulliken spin densities of the optimized Cu(II) complexes are reported in Table S2 (Supporting Information). Examples of B3LYP/6-31G(d) optimized Cu(II) complexes **1**, X**:** = dimethyl sulfide, $(CH_3)_2S$, are depicted in Figure 1.

The geometries of the Cu(II) complexes **3**−**7** (not shown; see Supporting Information) are similar to those observed for **1** (X**:** = $(CH_3)_2S$). B3LYP/6-31G(d) geometry optimization produces structures that are distorted square planar. The most evident difference among the **a**−**h** species is that as the number of nitrogen ligands on Cu(II) decreases so does the Cu(II)−X distance, irrespective of the nature of X**:**, by up to ~0.1 Å. There is a corresponding increase in the spin density on X**:** as the number of water ligands increases. A further variation in the spin densities on X**:** is dependent on the type of ligand trans to the Cu−X bond. If water is trans to X**:**, then the spin density on X**:** is greater than if ammonia is in this position.

Differences from the above pattern are apparent in the geometries of the thiolate complexes **2**, X**:** = CH_3S^-, shown in Figure 2. The most noticeable dissimilarity between the CH_3S^- species and the Cu(II) complexes of the other ligands, e.g., Figure 1, is that **2c**, **2e**, and **2h** are essentially trigonal about the copper with water in an axial position. The **2c**, **2e**, and **2h** structures resemble type-1 copper sites found in copper proteins, which have Cu−His_2Cys coordination.[e.g.,23,24] The $(CH_3)_2S$, and other species, and the **2a**, **2b**, and **2f** complexes have a distorted square planar arrangement at the copper. Second, the spin density is markedly higher on sulfur (up to 45%) and lower on copper when X**:** = CH_3S^- compared to $(CH_3)_2S$. The third difference lies in Cu−S distance, which is significantly shorter (~0.2 Å) in the thiolate species.

To determine if the axial water molecule in **2c**, **2e**, and **2h** was truly bound to the copper, these species were reoptimized after removal of the water. The resultant tricoordinate complexes are shown in Figure 3. Removal of the axial H_2O produces

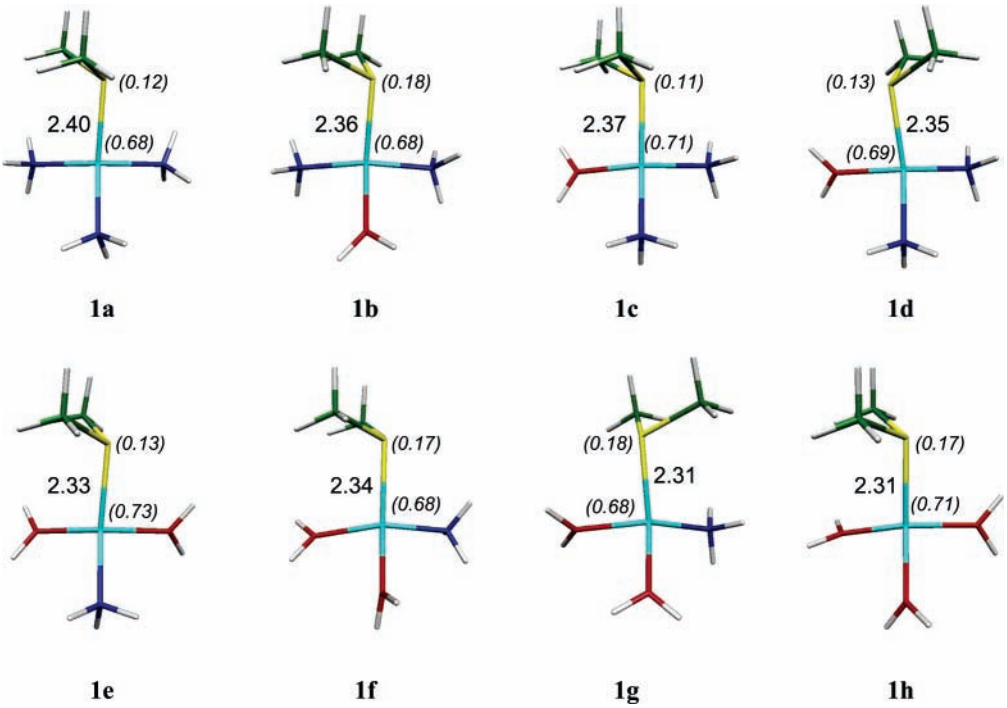

Figure 1. B3LYP/6-31G(d) optimized geometries and numbering system for $(NH_3)_i(H_2O)_{3-i}Cu(II)-S(CH_3)_2$ (i = 3, 2, 1, 0) complexes. Bond lengths given in angstroms. Italicized numbers in parentheses are Mulliken spin densities.

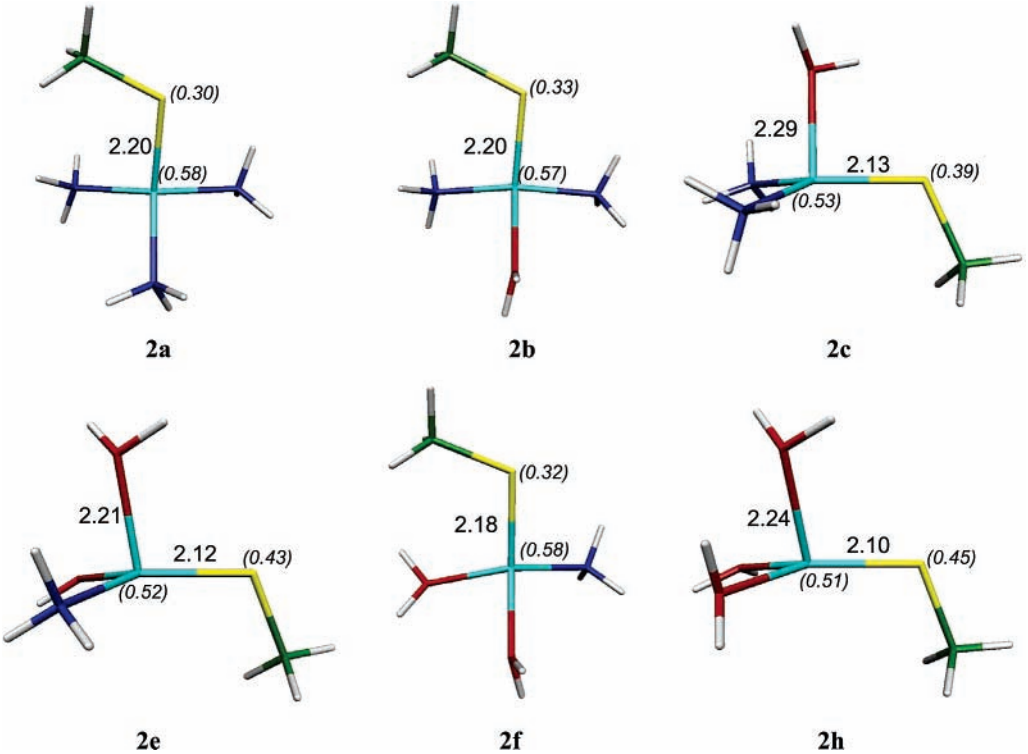

Figure 2. B3LYP/6-31G(d) optimized geometries and numbering system for $(NH_3)_i(H_2O)_{3-i}Cu(II)-SCH_3$ (i = 3, 2, 1, 0) complexes. Bond lengths given in angstroms. Italicized numbers in parentheses are Mulliken spin densities.

species that are trigonal and planar with small decreases in the Cu−S distances compared to the tetracoordinate complexes. There are also increases and decreases of ∼5% in the spin density on sulfur and copper, respectively. The binding affinity of the H_2O was then calculated as the free energy change in aqueous solution for reaction 2

$$(NH_3)_i(H_2O)_{3-i}Cu(II)-SCH_3 \rightarrow (NH_3)_i(H_2O)_{2-i}Cu(II) - SCH_3 + H_2O \quad (2)$$

where i = 2, 1, 0. The enthalpy, entropy, and free energy changes for reaction 2 are reported in Table 2, and for completeness, the losses of a water ligand from species **2b** and **2f** are included. The loss of water is exergonic in aqueous solution for all the thiolate tetracoordinate species. Closer inspection of Table 2 reveals that, for the trigonal pyramidal complexes **2c**, **2e**, and **2h**, the positive entropy change on going from one species to two is only enough to overcome the endothermicity of reaction 2 for **2c**. It is the −28 to −32 kJ

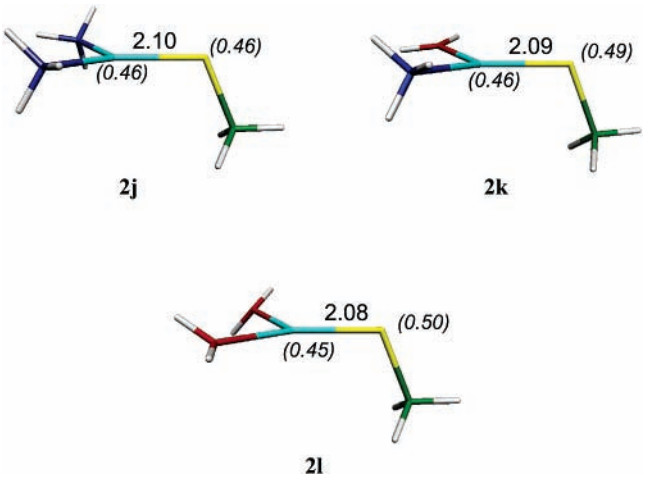

Figure 3. B3LYP/6-31G(d) optimized geometries for $(NH_3)_i(H_2O)_{2-i}$-Cu(II)−SCH_3 ($i = 2, 1, 0$) complexes. Bond lengths given in angstroms. Italicized numbers in parentheses are Mulliken spin densities.

TABLE 2: Energy Changes (kJ mol^{-1}): $(NH_3)_i(H_2O)_{3-i}Cu(II)-SCH_3 \rightarrow (NH_3)_i(H_2O)_{2-i}Cu(II)-SCH_3 + H_2O$ (reaction 2)[a]

reaction	ΔH (0 K)$_{(g)}$[b]	$\Delta H°$ (298 K)$_{(g)}$[b]	$T\Delta S$	$\Delta G_{(g)}$	$\Delta\Delta G_{solv}$	$\Delta G°_{(aq)}$[c]
2b → **2j** + H_2O	8.5	10.3	32.7	−22.5	−8.7	−31.1
2c → **2j** + H_2O	25.3	27.6	33.6	−6.0	−29.2	−35.2
2e → **2k** + H_2O	31.7	33.4	30.1	3.3	−28.3	−24.9
2f → **2k** + H_2O	8.0	11.0	35.9	−24.9	−6.2	−31.2
2h → **2l** + H_2O	38.9	41.8	33.4	8.4	−32.1	−23.7

[a] The standard state for all entropies and gas-phase free energies is 1 M at 298 K. [b] Enthalpies derived from the B3LYP/6-311+G(2df,2p)//B3LYP/6-31G(d) energies. [c] All species are 1 M except H_2O = 55.6 M.

mol^{-1} increase in the free energy of solvation that leads to the favorable free energy change in solution for the loss of the water molecule. This value is partially made up of the free energy of solvation for a water molecule, adjusted to account for the concentration (55.6 M) of liquid water, −16.4 kJ mol^{-1}.[41] The pattern is different for the loss of water from the distorted square planar complexes, **2b** and **2f**. Reaction 2 involving **2b** and **2f** remains endothermic in the gas phase, $\Delta H° \approx 10-11$ kJ mol^{-1}, compared to the $\Delta H° \approx 28-42$ kJ mol^{-1} values calculated for **2c**, **2e**, and **2h**. Since the entropy contribution to the free energy is similar for removal of H_2O from **2b**−**2h**, reaction 2 becomes exergonic in the gas phase for **2b** and **2f**. The much smaller increases in the free energy of solvation for reaction 2 of **2b** and **2f** compared to **2c**, **2e**, and **2h** means that for **2b** and **2f** the exergonicity predominantly arises from the gas-phase energy changes. These results indicate that although **2b** and **2f** are local minima it is energetically favorable for them to lose a water ligand and adopt a trigonal geometry both in the gas and aqueous phases. However, to ensure consistency and allow for direct comparison with the other ligands X**:**, the binding affinities for CH_3S^- have been determined using the tetracoordinate species. The calculated binding affinities will therefore be the upper boundary values for X**:** = CH_3S^-.

Complexes **5** (X**:** = MeImid) have the MeImid binding to Cu(II) through the Nπ of the imidazole. At the present level of theory, the difference in free energies in aqueous solution of the Nπ and Nτ protonated forms of MeImid is 1.5 kJ mol^{-1}, meaning both species are likely to be present in solution. The Cu(II) binding affinities of the two MeImid isomers should therefore be very similar, so in order to avoid duplication, it was decided to only include one set of Cu(II)−MeImid complexes in the current study. The rationale for choosing to examine the Nπ−Cu bound complexes came from experimental studies of the binding of Cu(II) to Aβ through the imidazole group of histidine. It has been found that the binding mode is pH dependent. At physiological pH, the favored binding mode to Cu(II) for histidine residues in Aβ is through Nπ.[16,19] It should be noted that in many copper proteins histidine residues bind to copper through the Nτ of the imidazole[57,58] and also that in a recent study Tickler et al. showed global methylation of either the Nπ or Nτ of histidines in Aβ did not preclude Cu(II) binding to Aβ.[59]

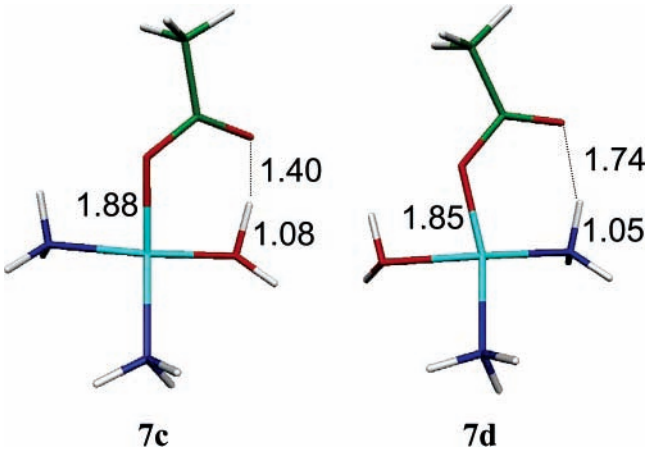

Figure 4. B3LYP/6-31G(d) optimized geometries for $(NH_3)_2$-(H_2O)Cu(II)−$CH_3CO_2^-$ cis complexes. Bond lengths given in angstroms.

In the case of complexes **7**, where X**:** = $CH_3CO_2^-$, there are large geometrical differences between the Cu(II) species that are dependent upon whether the acetate is oriented toward a water or ammonia ligand (see Figure 4). The acetate oxygen not bound to copper in **7c** forms a very short hydrogen bond (1.40 Å) to a water hydrogen and a significantly longer hydrogen bond (1.74 Å) to an ammonia hydrogen in **7d**. There is also elongation of both the HO−H and H_2N−H bonds upon formation of a hydrogen bond to the acetate oxygen to 1.08 Å from 0.97 Å and 1.05 Å from 1.02 Å, respectively.

The relative free energies in aqueous solution of the complexes that have both water and ammonia ligands, $i = 2$ (**b**−**d**, Scheme 1) and $i = 1$ (**e**−**g**, Scheme 1), are reported in Table 3. A trans effect is only evident when X**:** = $(CH_3)_2S$, and the effect is greatest for $i = 2$, with **1b** ≈ 18−20 kJ mol^{-1} more stable than **1c** and **1d** (Figure 1). The ammonia ligands prefer to be trans to each other and cis to $(CH_3)_2S$. This pattern is not seen for complexes **2** (X**:** = CH_3S^-), but this is to be expected, as there are large conformational changes between the **2b** and **2c** species and the **2e** and **2f** species that make such direct comparisons problematic. For complexes **4** (X**:** = CH_3NH_2) and **5** (X**:** = MeImid), the **b**,**c** and **d**,**e** isomers (Scheme 1) are very close in energy. While this was expected for X**:** = CH_3NH_2, since the ligands CH_3NH_2 and NH_3 are electronically very similar, it is not clear why it is also the case for X**:** = MeImid. In complexes **6** (X**:** = PhO^-), the relative free energies suggest that it is having an adjacent ammonia ligand interacting with the π-system of the phenolate group that stabilizes one isomer over another (e.g., **c** vs **d**, Scheme 1) rather than a trans effect. For complexes **7** (X**:** = $CH_3CO_2^-$), the more stable structures contain the strong hydrogen bond between acetate and water highlighted in Figure 4. The presence of this hydrogen bond appears to confer greater stability than a trans effect.

Cu(II)−Ligand Binding Affinities. The binding affinities, measured as the ability of X**:** to displace water, are shown in

TABLE 3: Relative Energies of the $(NH_3)_2(H_2O)Cu(II)-X$ and $(NH_3)(H_2O)_2Cu(II)-X$ complexes (kJ mol^{-1})[a]

$(NH_3)_2(H_2O)Cu(II)-X$							$(NH_3)(H_2O)_2Cu(II)-X$						
species[b]	ΔH (0 K)$_{(g)}$[c]	$\Delta H°$ (298 K)$_{(g)}$[c]	$T\Delta S$	$\Delta G_{(g)}$	$\Delta\Delta G_{solv}$	$\Delta G°_{(aq)}$	species[b]	ΔH (0 K)$_{(g)}$[c]	$\Delta H°$ (298 K)$_{(g)}$[c]	$T\Delta S$	$\Delta G_{(g)}$	$\Delta\Delta G_{solv}$	$\Delta G°_{(aq)}$
1b	0	0	0	0	0	0	**1e**	11.3	11.6	0.9	10.7	−1.7	9.0
1c	21.0	20.5	−1.2	21.7	−1.5	20.2	**1f**	0	0	0	0	0	0
1d	15.4	14.7	−3.5	18.2	−0.5	17.7	**1g**	−1.5	−1.8	−1.3	−0.5	1.4	1.0
2b	0.0	0.0	0.0	0.0	0.0	0.0	**2e**	0.0	0.0	0.0	0.0	0.0	0.0
2c	−16.8	−17.3	−0.8	−16.4	20.5	4.1	**2f**	23.7	22.4	−5.8	28.3	−22.0	6.2
4b	−1.1	−1.3	−1.1	−0.2	0.5	0.3	**4e**	1.9	1.8	0.1	1.6	0.5	2.1
4c	0.0	0.0	0.0	0.0	0.0	0.0	**4f**	0.0	0.0	0.0	0.0	0.0	0.0
5b	0.9	1.4	2.5	−1.1	1.8	0.7	**5e**	0.0	0.0	0.0	0.0	0.0	0.0
5c	0.0	0.0	0.0	0.0	0.0	0.0	**5f**	−2.2	−2.3	0.9	−3.2	3.8	0.6
6b	0.0	0.0	0.0	0.0	0.0	0.0	**6e**	4.7	3.6	−3.9	7.6	3.4	11.0
6c	1.8	−0.4	−6.7	6.3	4.6	10.9	**6f**	8.7	8.1	−2.7	10.9	2.2	13.0
6d	−4.5	−5.8	−2.6	−3.2	3.5	0.2	**6g**	0.0	0.0	0.0	0.0	0.0	0.0
7b	27.8	29.9	4.5	25.4	−6.8	18.6	**7e**	−1.6	−2.3	−2.9	0.5	4.7	5.2
7c	0.0	0.0	0.0	0.0	0.0	0.0	**7f**	0.0	0.0	0.0	0.0	0.0	0.0
7d	23.1	23.5	−0.5	24.0	−3.4	20.7	**7g**	25.2	26.1	0.1	26.0	−3.5	22.5

[a] The standard state for all entropies and free energies is 1 M at 298 K. [b] **1** X**:** = $(CH_3)_2S$; **2** X**:** = CH_3S^-; **4** X**:** = CH_3NH_2; **5** X**:** = MeImid; **6** X**:** = PhO^-; **7** X**:** = $CH_3CO_2^-$. See Scheme 1 for letter notation. [c] Enthalpies derived from the B3LYP/6-311+G(2df,2p)//B3LYP/6-31G(d) energies.

Figure 5. The binding affinities for the ligands X**:** = $(CH_3)_2S$ **1**, MeImid **5**, and $CH_3CO_2^-$ **7** with Cu(II) have been calculated as the free energies for reaction 3 occurring in aqueous solution.

$$(NH_3)_i(H_2O)_{3-i}Cu(II)-H_2O + X: \rightarrow (NH_3)_i(H_2O)_{3-i}Cu(II) - X + H_2O \quad (3)$$

where $i = 3, 2, 1, 0$; i.e., the ligand X**:** displaces a water molecule from the Cu(II) coordination sphere, and both reactant and product Cu(II) complexes are tetracoordinate. The aim of the present study has been to use these model Cu(II)−ligand complexes to gain insight into the binding of Cu(II) with ligands in biological systems, where such processes would occur at ∼pH 7. The conjugate acids of the ligands X**:** = CH_3S^- **2**, CH_3NH_2 **4**, and PhO^- **6** have pK_a's of 10.3, 10.64, and 9.95, respectively. Since the pK_a's of these ligands are greater than 7, they have been used in their protonated form in all calculations. The binding affinities for these ligands have therefore been calculated as the free energies in aqueous solution for eq 4

$$(NH_3)_i(H_2O)_{3-i}Cu(II) - H_2O + XH \rightarrow (NH_3)_i(H_2O)_{3-i}Cu(II) - X + H_2O + H^+ \quad (4)$$

Reaction 4 is pH-dependent because of the production of protons when XH is deprotonated and binds to Cu(II). To calculate the free energies for reaction 4 at the biologically relevant pH 7, the concentrations of the individual species must be taken into account. It has been assumed that the concentrations of the $(NH_3)_i(H_2O)_{3-i}Cu(II)-H_2O$ and $(NH_3)_i(H_2O)_{3-i}Cu(II)-X$ complexes are pH-independent and therefore 1 M; the displaced water molecule is treated as solvent, while at pH 7, $[H^+]$ would be 10^{-7} M. The concentrations of the XH for X**:** = CH_3S^-, CH_3NH_2, and PhO^- species are essentially 1 M, as their pK_a's are large enough that at pH 7 the protonated form would be present in >99% abundance. The free energy for reaction 4 at pH 7 has been denoted $\Delta G°'_{(aq)}$ and calculated using $\Delta G°'_{(aq)} = \Delta G°_{(aq)} + RT \ln Q$ where the reaction quotient, Q, simplifies to $[H^+]$ as all other relevant species are 1 M at pH 7. Hereafter, the symbol $\Delta G°'_{(aq)}$ will be used in a generic sense for free energies of reaction in aqueous solution; thus, for a reaction that is not pH-dependent, $\Delta G°'_{(aq)} = \Delta G°_{(aq)}$.

The binding affinities of the ligands X**:** determined from reactions 3 and 4 are presented as free energies in aqueous solution at pH 7 ($\Delta G°'_{(aq)}$) in Figure 5a,b. Binding affinities for complexes **3** have been omitted from all figures. This is because NH_3 and CH_3NH_2 are electronically similar and yield comparable affinities. Figure 5a displays the binding affinities for reactions 3 and 4 where $i = 3, 2$ (cases a to d, Scheme 1) and Figure 5b for $i = 1, 0$ (cases e to h, Scheme 1). The first general trend observable in Figure 5a,b is that as the number of water ligands attached to Cu(II) increases then so does the binding affinity of the ligand X**:**, irrespective of the identity of X**:**. The greatest binding affinities are therefore seen for the displacement of water from the $Cu(II)(H_2O)_4$ species (the solid curve h in Figure 5b). CH_3S^- has the highest affinity, −53.5 kJ mol^{-1}. The next highest affinities are obtained for MeImid and $CH_3CO_2^-$, −35.2 and −32.4 kJ mol^{-1}, respectively. The binding affinity for the MeImid species where Nπ is protonated and Nτ binds to the copper in the $(H_2O)_3Cu(II)-MeImid(N\tau)$ complex has also been calculated. The binding affinity is −40.9 kJ mol^{-1} for this Cu(II) binding mode of 4-CH_3-imidazole. This result agrees with recent experimental data that indicates that the binding of Cu^{2+} to N-methylated histidine side chains is stronger if the copper is bound to the Nτ rather than the Nπ atom of the imidazole ring.[59] Each of the ligands X**:**, except $(CH_3)_2S$, will displace water from an aqueous Cu^{2+} ion. In this case, the binding affinity of X**:** could also be thought of as the first attachment of an aqueous Cu^{2+} ion to a peptide.

The nature of X**:** determines its sensitivity to the Cu(II) environment (Figure 5a,b). Complexes **4** and **5**, with nitrogen ligands CH_3NH_2 and MeImid, exhibit the least variation (∼15 kJ mol^{-1}) in binding affinities over the range of Cu(II) environments. For complexes **1** (X**:** = $(CH_3)_2S$), the binding affinities vary over a range of ∼25 kJ mol^{-1}; for **6** (X**:** = PhO^-), the range is ∼30 kJ mol^{-1}; and for **2** (X**:** = CH_3S^-) and **7** (X**:** = $CH_3CO_2^-$), they differ by up to ∼45 kJ mol^{-1}. The $CH_3CO_2^-$ binding affinities are grouped into two subsets, those for complexes where the acetate hydrogen bonds to an ammonia proton and those when it is hydrogen-bonded to water, and it is this latter set for which the binding affinities are greater.

The relative binding affinities of the various ligands vary with the Cu(II) environment. In Figure 5a, when the three other ligands are all NH_3 (case a in Scheme 1), the binding affinities of X**:** are in the order MeImid > CH_3S^- > CH_3NH_2 > $CH_3CO_2^-$ > $(CH_3)_2S$ > PhO^-. The trend is almost the same when there is a single water and two NH_3 ligands (cases b−d,

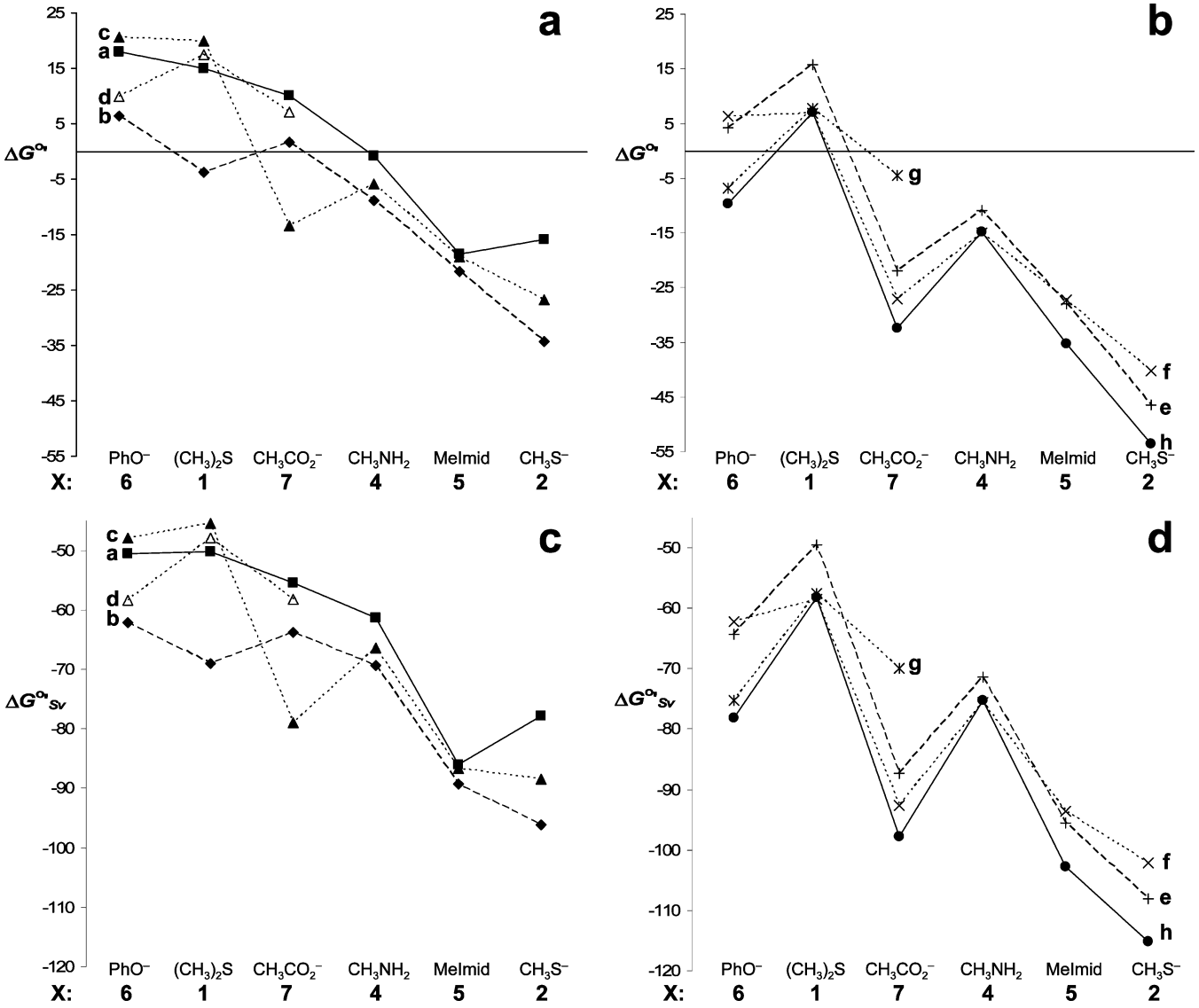

Figure 5. (a, b**)** Free energies in aqueous solution at pH 7 ($\Delta G^{\circ\prime}$) (kJ mol^{-1}) for the reactions $(NH_3)_i(H_2O)_{3-i}Cu(II)-H_2O + X\text{:} \rightarrow (NH_3)_i(H_2O)_{3-i}$-Cu(II)$-X + H_2O$ where X**:** = $(CH_3)_2S$, MeImid, $CH_3CO_2^-$, and $(NH_3)_i(H_2O)_{3-i}Cu(II)-H_2O + XH \rightarrow (NH_3)_i(H_2O)_{3-i}Cu(II)-X + H_2O + H^+$ where X**:** = CH_3S^-, CH_3NH_2, PhO^-. (c, d) Free energies in aqueous solution at pH 7 ($\Delta G^{\circ\prime}_{Sv}$) (kJ mol^{-1}) (see text for details). (a, c) (■) $i = 3$ (a), (◆) $i = 2$ (b), (▲) $i = 2$ (c), (△) $i = 2$ (d). (b, d) (+) $i = 1$ (e), (×) $i = 1$ (f), (∗) $i = 1$ (g), (●) $i = 0$ (h).

Scheme 1) except that CH_3S^- gives higher affinities than MeImid in these cases. There are two points in Figure 5a that do not follow this trend and give larger binding affinities. The first is for the **1b** (X**:** = $(CH_3)_2S$) complex with water in the trans position. This is the only dimethyl sulfide species that has a small negative free energy (−4 kJ mol^{-1}) for the displacement of water. It is not clear why this is a special case, since other $(CH_3)_2S-Cu(II)$ species have an S−Cu−O trans motif. The larger binding affinity may be a consequence of having the above motif in conjunction with two ammonia ligands trans to each other. The second species with a greater binding affinity than would be estimated from the general trend is **7c** (X**:** = $CH_3CO_2^-$), but this is due to the strong hydrogen bond formed between acetate and water, as shown in Figure 4.

The relative binding affinities shown in Figure 5b exhibit a slightly different pattern for the $(NH_3)(H_2O)_2Cu(II)-X$ (curves e−g) and $(H_2O)_3Cu(II)-X$ (curve h) complexes. The binding affinities for **7** (X**:** = $CH_3CO_2^-$) are greater than those for **4** (X**:** = CH_3NH_2), but again, this is a result of the strong hydrogen bond between acetate and a water ligand on Cu(II). The binding affinities for **6** (X**:** = PhO^-) become larger than those for **1** (X**:** = $(CH_3)_2S$), and as the Cu(II) environment moves toward that of an aqueous Cu^{2+} ion, it is favorable for PhO^- to displace water from Cu(II). In all but the $(NH_3)_3Cu(II)-X$ copper environment, complexes **2** (X**:** = CH_3S^-) have the greatest binding affinities. As discussed above, the binding affinities for X**:** = CH_3S^- will be upper limits, as the $Cu(II)-SCH_3$ complexes have been treated as tetracoordinate species.

The binding affinities shown in Figure 5a,b are for the displacement of water from the Cu(II) coordination sphere by the ligand X**:**. These affinities do not take into account the effect that the presence of X**:** bound to the copper may have on the subsequent displacement of water from the Cu(II) coordination sphere by other ligands. To explore this effect, the data for the X**:** = $(CH_3)_2S$, MeImid, and $CH_3CO_2^-$ complexes have been reanalyzed. This subset of ligands was chosen because the binding affinities for MeImid and $CH_3CO_2^-$ are similar for the displacement of water from an aqueous Cu^{2+} ion. The effect of these ligands on water displacement reactions from the $(H_2O)_3$-Cu(II)$-X$ species may help determine which would be the preferred ligand for Cu^{2+}. $(CH_3)_2S$ was also used because it is the model for a methionine side chain, a residue of partic-

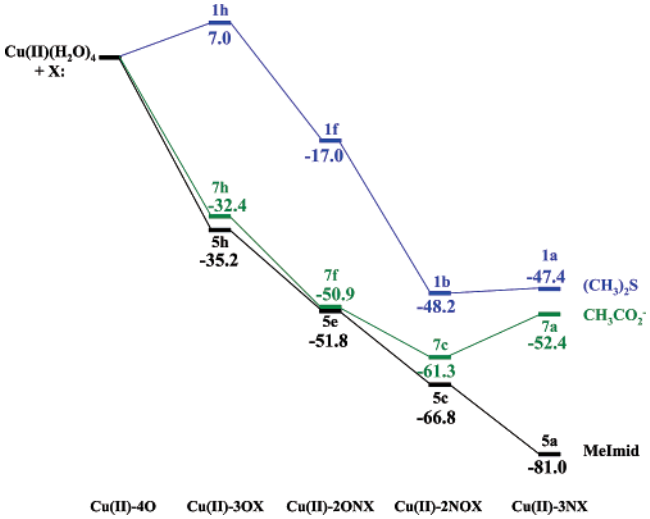

Figure 6. Relative free energies in aqueous solution at pH 7 ($\Delta G^{\circ\prime}$) (kJ mol^{-1}) for initial binding of X**:** to Cu(II)$(H_2O)_4$ followed by successive displacements of H_2O by NH_3 from the Cu(II) coordination sphere. X**:** = $(CH_3)_2S$, MeImid, and $CH_3CO_2^-$.

ular interest in Aβ. This effect has been examined by calculating the free energies in aqueous solution for the successive replacement of water ligands from the $(H_2O)_3Cu(II)-X$ complexes by ammonia, our generic model nitrogen ligand (Figure 6)

$$(NH_3)_i(H_2O)_{3-i}Cu(II)-X + NH_4^+ \rightarrow (NH_3)_{i+1}(H_2O)_{2-i}Cu(II)-X + H_2O + H^+ \quad (5)$$

where $i = 0, 1, 2$. The free energy changes at pH 7 for the initial attachment of X**:** to aqueous Cu^{2+}, plus consecutive displacements of water via reaction 5 are shown in Figure 6. The free energies are all shown relative to the separate Cu(II)-$(H_2O)_4$ + X**:** species and represent the lowest-energy path for each ligand X**:**. More detailed energetic data can be found in Table S5 (Supporting Information). The free energies in Figure 6 show that, for the first and second displacements of water from an aqueous Cu^{2+} ion, MeImid and $CH_3CO_2^-$ have comparable energy changes. The energy difference is slightly increased to 5.5 kJ mol^{-1} for displacement of a third water, favoring MeImid over $CH_3CO_2^-$. The replacement of the final H_2O by NH_3 is exergonic by 14 kJ mol^{-1} for MeImid but endergonic by 9 kJ mol^{-1} for $CH_3CO_2^-$. The endergonicity of the final step in Figure 6 for $CH_3CO_2^-$ is caused by the loss of the strong hydrogen bond between the acetate and the water molecule that is displaced. The energy profile for X**:** = $(CH_3)_2S$ shows a step up in energy for the initial binding of $(CH_3)_2S$ to aqueous Cu^{2+}, followed by exergonic reactions for displacement of two further water molecules. The final replacement of H_2O by NH_3 is effectively energetically neutral when X**:** = $(CH_3)_2S$. At each step in Figure 6, the $(CH_3)_2S$ species are considerably higher in energy than the MeImid and $CH_3CO_2^-$ complexes. Although as the number of nitrogen ligands of Cu(II) increases, the $(CH_3)_2S$ and $CH_3CO_2^-$ energies become closer and for the endpoints of the pathways are only 5 kJ mol^{-1} apart. The energy profiles in Figure 6 indicate that Cu^{2+} will preferentially bind MeImid over $(CH_3)_2S$ and $CH_3CO_2^-$, particularly once the Cu(II) has two or more nitrogen ligands present in its coordination sphere. It is also noticeable that, after the initial binding of MeImid to aqueous Cu^{2+}, the free energy changes for successive displacements of water by NH_3 are fairly constant. This is not the case for $(CH_3)_2S$ and $CH_3CO_2^-$: These ligands appear to affect the coordination of nitrogen ligands to Cu(II) to a greater extent than MeImid.

Cu(II)−Ligand Binding Affinities − Implications for Aβ. In peptides, the residue side chains that would form the coordination sphere of the Cu(II) would not have the free range of motion of the model ligands X**:**, because of restrictions imposed by the protein secondary structure. In an attempt to gain insight into the effect of the reduction in the degrees of freedom on the binding affinities of these ligands in a peptide, the free energies for reactions 3 and 4 have been reevaluated with the translational and rotational components of the entropy removed for all species except the H_2O molecule displaced by X**:**. This is a crude approximation and represents a limiting case, as the binding affinities are for a situation where the species involved have only vibrational degrees of freedom. The real environment within a protein will occur at some point between the two situations presented here.

The recalculated free energies in aqueous solution at pH 7 ($\Delta G^{\circ\prime}_{Sv}$) are displayed in Figure 5c,d. The reevaluated energetics for reactions 3 and 4 are reported in Table S4 (Supporting Information). The binding affinities for all ligands X**:** are increased by ~60−65 kJ mol^{-1}. Consequently, $\Delta G^{\circ\prime}_{Sv}$ is negative, and all ligands X**:** will displace water from the Cu(II) coordination sphere.

The calculated binding affinities suggest that Aβ, lacking a cysteine residue (modeled by CH_3S^-), would preferentially bind Cu(II) at a histidine. This is in qualitative agreement with experiment, since most copper-binding proteins have multiple histidine residues bound to copper.[e.g.,25,60,61] It is also in agreement with the copper-binding data for Aβ, for which 3N1O and 4N copper-binding environments have been proposed where the majority of the nitrogen ligands are thought to come from histidine residues. Recent evidence indicates that the N-terminus is also important for copper binding to Aβ.[12,14,15] In the 3N1O case, this would suggest two histidines and the N-terminus as the nitrogen ligands, plus an oxygen ligand. The calculated binding affinities would not rule out this combination, although they indicate that histidine binds to Cu(II) more strongly than lysine/N-terminus, whatever the existing ligand environment of the copper. In fact, in the entropy-constrained systems, the difference in His and N-terminus model binding affinities increases. The binding of the N-terminus over the third His in Aβ to Cu(II) would therefore likely be the result of peptide secondary structure considerations. The oxygen ligand has been postulated to be the tyrosine at position 10 in Aβ.[16,17] However, the current calculations do not support this, since the tyrosine model, PhO^-, exhibits some of the lowest binding affinities for the ligands studied. If Tyr10 is ligated to Cu(II) in Aβ, then it appears that this would also be a consequence of secondary structure restrictions rather than a preference of the Cu(II) to bind to tyrosine. This is in agreement with the conclusions of Karr et al. who discount tyrosine as a ligand of copper in the Cu(II)/Aβ complex.[14] The calculated binding affinities indicate that oxygen ligands such as glutamic or aspartic acid, modeled by $CH_3CO_2^-$, are more likely to provide a fourth ligand of the Cu(II) coordination sphere. An alternative possibility is that a peptide backbone carbonyl oxygen is ligated to copper. This situation will be described in detail in a forthcoming paper.[62]

A 4N arrangement of ligands in the Cu(II)/Aβ complex has also been proposed,[12,16] with all three histidine residues in monomeric Aβ (positions 6, 13, and 14) bound to Cu(II). The fourth Cu(II) ligand must come from a different residue, either from the same Aβ or from another Aβ strand. On the basis of the above results, the most likely choice of nitrogen ligand from

a single Aβ molecule would be either a lysine or the N-terminus of Aβ. A further possibility would involve the Cu(II) binding to more than one Aβ, and in this case, all four nitrogen ligands could be histidine.

The possibility of methionine (Met35) being a ligand of copper in Aβ appears unlikely from examination of the calculated relative binding affinities, although it may be competitive with lysine or the N-terminus in a Cu(II) environment with two nitrogen ligands trans to each other and an oxygen trans to the methionine sulfur (case b, Scheme 1). This is in agreement with experiment, insofar as methionine has not been observed in the Cu(II) coordination sphere of Aβ, and with a theoretical investigation of the binding of Cu(II) to the Met region of a polypeptide.[63]

It has been shown that homocysteine potentiates copper and Aβ mediated toxicity in neuronal cultures and that reduction of Cu(II) to Cu(I) is a requirement for this to occur.[30] The calculations, using CH_3S^- as a model, suggest that if homocysteine were present then it would displace any of the residues present in Aβ to ligate to the Cu(II). The high degree of spin transfer shown in Figure 2 suggests that it could spontaneously reduce the copper to Cu(I) in the process. The reduction potentials of the Cu(II) complexes discussed in this paper and the structures and stabilities of the corresponding Cu(I) species are the subject of a forthcoming publication.[64]

Conclusions

A comparative study of the binding affinities of the ligands X**:** = $(CH_3)_2S$, CH_3S^-, CH_3NH_2, MeImid, PhO^-, and $CH_3CO_2^-$ to Cu(II) in the distorted square planar model complexes $(NH_3)_i(H_2O)_{3-i}Cu(II)-H_2O$ (i = 3, 2, 1, 0) has been performed. The calculated relative binding affinities at pH 7 give the following orders: MeImid > CH_3S^- > CH_3NH_2 > $CH_3CO_2^-$ > $(CH_3)_2S$ > PhO^- for i = 3, CH_3S^- > MeImid > CH_3NH_2 > $CH_3CO_2^-$ > $(CH_3)_2S$ > PhO^- for i = 2, and CH_3S^- > MeImid > $CH_3CO_2^-$ > CH_3NH_2 > PhO^- > $(CH_3)_2S$ for i = 1, 0. The greatest Cu(II)−X free energies of binding are computed for i = 0, which models the binding of X**:** to an aqueous Cu^{2+} ion, with the displacement of one of the coordinated water molecules.

The calculated binding affinities for Cu(II) show that CH_3S^- is an excellent ligand for Cu(II), $\Delta G^{\circ\prime}_{(aq)} = -16.0$ to -53.5 kJ mol^{-1}. MeImid gives the next highest affinities for Cu(II), $\Delta G^{\circ\prime}_{(aq)} = -18.5$ to -35.2 kJ mol^{-1}. $CH_3CO_2^-$ can be a good Cu(II) ligand under the specific circumstance of having an adjacent OH group bound to the copper that can hydrogen bond to the free acetate oxygen, $\Delta G^{\circ\prime}_{(aq)} = -13.5$ to -32.4 kJ mol^{-1}. It is a poor Cu(II) ligand when this interaction is not present, $\Delta G^{\circ\prime}_{(aq)} = 10.1$ to -4.6 kJ mol^{-1}. MeImid is the most favored ligand for Cu(II), despite competition with $CH_3CO_2^-$, when successive displacements of H_2O from the Cu(II) coordination sphere are considered. The calculated binding affinities also show that $(CH_3)_2S$ and PhO^- are poor ligands for Cu(II), $\Delta G^{\circ\prime}_{(aq)} = 19.8$ to -3.7 kJ mol^{-1} and $\Delta G^{\circ\prime}_{(aq)} = 20.6$ to -9.7 kJ mol^{-1}, respectively.

When extrapolated to the binding of Cu(II) to Aβ, the calculations suggest that Cu(II) would preferentially bind to the histidine residues. In the case of monomeric Aβ, if all three histidine residues are consecutively coordinated, then coordination of the fourth ligand would likely involve a lysine or the N-terminus. If the fourth ligand has oxygen bound to copper, then it would be more probable for this to be from a glutamate or aspartate residue side chain, rather than the tyrosine at position 10. Methionine appears unlikely to be a Cu(II) ligand in Aβ, but any cysteine or homocysteine present would bind to Cu(II) more strongly than any of the above residues.

Acknowledgment. This work was supported by grants from the Natural Sciences and Engineering Council (NSERC) of Canada and the Alzheimer's Society of Canada. This research has also been enabled by the use of WestGrid computing resources, which are funded in part by the Canada Foundation for Innovation, Alberta Innovation and Science, BC Advanced Education, and the participating research institutions. WestGrid equipment is provided by IBM, Hewlett-Packard, and SGI. P.B. acknowledges the Alberta Ingenuity Fund for the provision of a graduate studentship.

Supporting Information Available: Table S1 contains the primary thermodynamic data for all species considered in the present work. Table S2 contains selected structural parameters and B3LYP/6-31G(d) Mulliken spin densities for species **1** to **7**. Tables S3−S5 contain the numerical data for reactions 3−5. Table S6 contains the Cartesian coordinates for the B3LYP/6-31G(d) optimized geometries of all species. This material is available free of charge via the Internet at http://pubs.acs.org.

References and Notes

(1) Selkoe, D. J. *J. Biol. Chem.* **1996**, *271*, 18295−18298.
(2) Varadarajan, S.; Yatin, S.; Aksenova, M.; Butterfield, D. A. *J. Struct. Biol.* **2000**, *130*, 184−208.
(3) Lovell, M. A.; Robertson, J. D.; Teesdale, W. J.; Campbell, J. L.; Markesbery, W. R. *J. Neurol. Sci.* **1998**, *158*, 47−52.
(4) Bush, A. I.; Pettingell, W. H.; Multhaup, G.; Paradis, M. D.; Vonsattel, J.-P.; Gusella, J. F.; Beyreuther, K.; Masters, C. L.; Tanzi, R. E. *Science* **1994**, *265*, 1464−1467.
(5) Curtain, C. C.; Ali, F.; Volitakis, I.; Cherny, R. A.; Norton, R. S.; Beyreuther, K.; Barrow, C. J.; Masters, C. L.; Bush, A. I.; Barnham, K. J. *J. Biol. Chem.* **2001**, *276*, 20466−20473.
(6) Atwood, C. S.; Moir, R. D.; Huang, X.; Scarpa, R. C.; Bacarra, N. M. E.; Romano, D. M.; Hartshorn, M. A.; Tanzi, R. E.; Bush, A. I. *J. Biol. Chem.* **1998**, *273*, 12817−12826.
(7) Huang, X.; Atwood, C. S.; Hartshorn, M. A.; Multhaup, G.; Goldstein, L. E.; Scarpa, R. C.; Cuajungco, M. P.; Gray, D. N.; Lim, J.; Moir, R. D.; Tanzi, R. E.; Bush, A. I. *Biochem.* **1999**, *38*, 7609−7616.
(8) Huang, X.; Cuajungco, M. P.; Atwood, C. S.; Hartshorn, M. A.; Tyndall, J. D. A.; Hanson, G. R.; Stokes, K. C.; Leopold, M.; Multhaup, G.; Goldstein, L. E.; Scarpa, R. C.; Saunders: A. J.; Lim, J.; Moir, R. D.; Glabe, C.; Bowden, E. F.; Masters, C. L.; Fairlie, D. P.; Tanzi, R. E.; Bush, A. I. *J. Biol. Chem.* **1999**, *274*, 37111−37116.
(9) Ali, F. E. A.; Barnham, K. J.; Barrow, C. J.; Separovic, F. *Aust. J. Chem.* **2004**, *57*, 511−518.
(10) Garzon-Rodriguez, W.; Yatsimirsky, A. K.; Glabe, C. G. *Bioorg. Med. Chem. Lett.* **1999**, *9*, 2243−2248.
(11) Atwood, C. S.; Scarpa, R. C.; Huang, X.; Moir, R. D.; Jones, W. D.; Fairlie, D. P.; Tanzi, R. E.; Bush, A. I. *J. Neurochem.* **2000**, *75*, 1219−1233.
(12) Syme, C. D.; Nadal, R. C.; Rigby, S. E. J.; Viles, J. H. *J. Biol. Chem.* **2004**, *279* (18), 18169−18177.
(13) Karr, J. W.; Kaupp, L. J.; Szalai, V. A. *J. Am. Chem. Soc.* **2004**, *126* (41), 13534−13538.
(14) Karr, J. W.; Akintoye, H.; Kaupp, L. J.; Szalai, V. A. *Biochem.* **2005**, *44*, 5437−5487.
(15) Kowalik-Jankowska, T.; Ruta, M.; Wiśniewska, K.; Łankiewicz, L.; Dyba, M *J. Inorg. Biochem.* **2004**, *98*, 940−950.
(16) Miura, T.; Suzuki, K.; Kohata, N.; Takeuchi, H. *Biochem.* **2000**, *39*, 7024−7031.
(17) Barnham, K. J.; Haeffner, F.; Ciccotosto, G. D.; Curtain, C. C.; Tew, D.; Mavros, C.; Beyreuther, K.; Carrington, D.; Masters, C. L.; Cherny, R. A.; Cappai, R.; Bush, A. I. *FASEB J.* **2004**, *18* (10), 1427−1429.
(18) Schöneich, C.; Williams, T. D. *Chem. Res. Toxicol.* **2002**, *15*, 717−722.
(19) Dong, J.; Atwood, C. S.; Anderson, V. E.; Siedlak, S. L.; Smith, M. A.; Perry, G.; Carey, P. R. *Biochem.* **2003**, *42*, 2768−2773.
(20) Butterfield, D. A.; Kanski, J. *Peptides* **2002**, *23*, 1299−1309.
(21) Kadlick, V.; Sicard-Roselli, C.; Mattioli, T. A.; Kodicek, M.; Houée-Levin, C. *Free Radical Biol. Med.* **2004**, *37*, 881−891.
(22) Yatin, S. M.; Varadarajan, S.; Link, C. D.; Butterfield, D. A. *Neurobiol. Aging* **1999**, *20*, 325−330.
(23) Inoue, T.; Sugawara, H.; Hamanaka, S.; Tsukui, H.; Suzuki, E.; Kohzuma, T.; Kai, Y. *Biochemistry* **1999**, *38*, 6063−6069.
(24) Nar, H.; Messerschmidt, R.; Huber, R.; van de Kamp, M.; Canters, G. W. *J. Mol. Biol.* **1991**, *221*, 765.

(25) Prigge, S. T.; Kolhekar, A. S.; Eipper, B. A.; Mains, R. E.; Amzel, L. M. *Science* **1997**, *278*, 1300−1305.
(26) Prigge, S. T.; Kolhekar, A. S.; Eipper, B. A.; Mains, R. E.; Amzel, L. M. *Nat. Struct. Biol.* **1999**, *6* (10), 976−983.
(27) Kruman, I. I.; Kumaravel, T. S.; Lohani, A.; Pedersen, W. A.; Cutler, R. G.; Kruman, Y.; Haughey, N.; Lee, J.; Evans, M.; Mattson, M. P. *J. Neurosci.* **2002**, *22*, 1752−1762.
(28) Mok, S. S.; Turner, B. J.; Beyreuther, K.; Masters, C. L.; Barrow, C. J.; Small, D. H. *Eur. J. Biochem.* **2002**, *269*, 3014−3022.
(29) Ho, P. I.; Collins, S. C.; Dhitavat, S.; Ortiz, D.; Ashline, D.; Rogers, E.; Shea, T. B. *J. Neurochem.* **2001**, *78*, 249−253.
(30) White, A. R.; Huang, H.; Jobling, M. F.; Barrow, C. J.; Beyreuther, K.; Masters, C. L.; Bush, A. I.; Cappai, R. *J. Neurochem.* **2001**, *76*, 1509−1520.
(31) Frisch, M. J.; Trucks, G. W.; Schlegel, H. B.; Scuseria, G. E.; Robb, M. A.; Cheeseman, J. R.; Montgomery, J. A., Jr.; Vreven, T.; Kudin, K. N.; Burant, J. C.; Millam, J. M.; Iyengar, S. S.; Tomasi, J.; Barone, V.; Mennucci, B.; Cossi, M.; Scalmani, G.; Rega, N.; Petersson, G. A.; Nakatsuji, H.; Hada, M.; Ehara, M.; Toyota, K.; Fukuda, R.; Hasegawa, J.; Ishida, M.; Nakajima, T.; Honda, Y.; Kitao, O.; Nakai, H.; Klene, M.; Li, X.; Knox, J. E.; Hratchian, H. P.; Cross, J. B.; Bakken, V.; Adamo, C.; Jaramillo, J.; Gomperts, R.; Stratmann, R. E.; Yazyev, O.; Austin, A. J.; Cammi, R.; Pomelli, C.; Ochterski, J. W.; Ayala, P. Y.; Morokuma, K.; Voth, G. A.; Salvador, P.; Dannenberg, J. J.; Zakrzewski, V. G.; Dapprich, S.; Daniels, A. D.; Strain, M. C.; Farkas, O.; Malick, D. K.; Rabuck, A. D.; Raghavachari, K.; Foresman, J. B.; Ortiz, J. V.; Cui, Q.; Baboul, A. G.; Clifford, S.; Cioslowski, J.; Stefanov, B. B.; Liu, G.; Liashenko, A.; Piskorz, P.; Komaromi, I.; Martin, R. L.; Fox, D. J.; Keith, T.; Al-Laham, M. A.; Peng, C. Y.; Nanayakkara, A.; Challacombe, M.; Gill, P. M. W.; Johnson, B.; Chen, W.; Wong, M. W.; Gonzalez, C.; Pople, J. A. *Gaussian 03*, revision B.05; Gaussian, Inc.: Wallingford, CT, 2004.
(32) Schaftenaar G.; Noordik, J. H. MOLDEN 4.3. *J. Comput.-Aided Mol. Des.* **2000**, *14*, 123−134
(33) Flükiger, P.; Lüthi, H. P.; Portmann, S.; Weber J. MOLEKEL 4.0, Swiss Center for Scientific Computing, Manno, Switzerland, 2000.
(34) Scott, A. P.; Radom, L. *J. Phys. Chem.* **1996**, *100*, 16502−16513.
(35) Klamt, A.; Schüürmann, G. *J. Chem. Soc., Perkin Trans.* **1993**, *2*, 799−805.
(36) Andzelm, J.; Kolmel, C.; Klamt, A. *J. Chem. Phys.* **1995**, *103*, 9312−9320.
(37) Barone, V.; Cossi, M. *J. Phys. Chem. A* **1998**, *102*, 1995−2001.
(38) Cossi, M.; Rega, N.; Scalmani, G.; Barone, V. *J. Comput. Chem.* **2003**, *24*, 669−681.
(39) Zhan, C.; Bentley, J.; Chipman, D. M. *J. Chem. Phys.* **1998**, *108*, 177−192.
(40) Leung, B. O.; Reid, D. L.; Armstrong, D. A.; Rauk, A. *J. Phys. Chem. A* **2004**, *108*, 2720−2725.
(41) Calculated as the difference between $\Delta_f G_{(g)}(H_2O)$ and $\Delta_f G_{(l)}(H_2O)$, corrected to the standard state of 1 M. The CPCM calculated value is $\Delta_f G_{solv}(H_2O) = -28.7$ kJ mol^{-1}.
(42) Liptak, M. D.; Gross, K. C.; Seybold, P. G.; Feldus, S.; Shields, G. C. *J. Am. Chem. Soc.* **2002**, *124*, 6421−6427.
(43) Brunelle, P.; Rauk, A. *J. Phys. Chem. A* **2004**, *108* (50), 11032−11041.
(44) Lu, Y.; Gralla, E. B.; Roe, J. A.; Valentine, J. S. *J. Am. Chem. Soc.* **1992**, *114*, 3560−3562.
(45) Andrew, C. R.; Yeom, H.; Valentine, J. S.; Karlsson, B. G.; Bonander, N.; van Pouderoyen, G.; Canters, G. W.; Loehr, T. M.; Sanders-Loehr, J. *J. Am. Chem. Soc.* **1994**, *116*, 11489−11498.
(46) den Blaauwen, T.; Hoitink, C. W. G.; Canters, G. W.; Han, J.; Loehr, T. M.; Sanders-Loehr, J. *Biochemistry* **1993**, *32*, 12455−12464.
(47) Rigo, A.; Corazza, A.; di Paolo, M. L.; Rossetto, M.; Ugolini, R.; Scarpa, M. *J. Inorg. Biochem.* **2004**, *98*, 1495−1501.
(48) Bagiyan, G. A.; Koroleva, I. K.; Soroka, N. V.; Ufimtsev, A. V. *Kinet. Katal.* **2004**, *45*, 372−380.
(49) Pawelec, M.; Stochel, G.; van Eldik, R. *J. Chem. Soc., Dalton Trans.* **2004**, 292−298.
(50) Bercer, A.; Nukada, T.; Margl, P.; Ziegler, T. *J. Phys. Chem. A* **1999**, *103*, 9693−9701.
(51) Pushie, M. J. M.Sc. Thesis, University of Calgary, 2002.
(52) Nomura, M.; Yamaguchi, T. *J. Phys. Chem.* **1988**, *92*, 6157.
(53) Powell, D. H.; Helm, L.; Merbach, A. E. *J. Chem. Phys.* **1991**, *95*, 9258.
(54) Richens, D. T. *The Chemistry of Aqua Ions*; Wiley: Chichester, UK, 1997.
(55) Pasquarello, A.; Petri, I.; Salmon, P. S.; Parisel, O.; Car, R.; Toth, E.; Powell, D. H.; Fischer, H. E.; Helm, L.; Merbach, A. E. *Science* **2001**, *291*, 856−859.
(56) *Stability constants of metal ion complexes*, Supplement 21; Chemical Society (Great Britain): London, U.K., 1982.
(57) Li, R.; Klinman, J. P.; Mathews, F. S. *Structure* **1998**, *6*, 293−307.
(58) Fusetti, F.; Schröter, K. H.; Steiner, R. A.; van Noort, P. I.; Pijning, T.; Rozeboom, H. J.; Kalk, K. H.; Egmond, M. R.; Dijkstra, B. W. *Structure* **2002**, *10*, 259−268.
(59) Tickler, A. K.; Smith, D. G.; Ciccotosto, G. D.; Tew, D. J.; Curtain, C. C.; Carrington, D.; Masters, C. L.; Bush, A. I.; Cherny, R. A.; Cappai, R.; Wade, J. D.; Barnham, K. J. *J. Biol. Chem.* **2005**, *280* (14), 13355−13363.
(60) Zaitseva, I.; Zaitsev, V.; Card, G.; Moshkov, K.; Bax, B.; Ralph, A.; Lindley, P. *J. Biol. Inorg. Chem.* **1996**, *1*, 15.23.
(61) Kaufman Katz, A.; Shimoni-Livay, L.; Navon, O.; Navon, N.; Bock, C. W.; Glusker, J. P. *Helv. Chim. Acta* **2003**, *86*, 1320−1338.
(62) Raffa, D. F.; Gomez-Balderas, R.; Brunelle, P.; Rickard, G. A.; Rauk, A. Manuscript in preparation.
(63) Gomez-Balderas, R.; Raffa, D. F.; Rickard, G. A.; Brunelle, P.; Rauk, A. *J. Phys. Chem. A* **2005**, *109*, 5498−5508.
(64) Rickard, G. A.; Gomez-Balderas, R.; Brunelle, P.; Raffa, D. F.; Rauk, A. Manuscript in preparation.